Optical Materials: X 12 (2021) 100088

Contents lists available at ScienceDirect

Optical Materials: X

journal homepage: www.journals.elsevier.com/optical-materials-x

(INVITED) Emerging routes to light-matter interaction in two-dimensional materials

C. Grazianetti [a,**], C. Martella [a,***], E. Cinquanta [b,*]

[a] CNR-IMM, Agrate Brianza Unit, Via C. Olivetti 2, Agrate Brianza, I-20864, Italy
[b] Istituto di Fotonica e Nanotecnologie, Consiglio Nazionale delle Ricerche, 20133, Milan, Italy

ARTICLE INFO

Keywords:
Xenes
Transition metal dichalcogenides
Photonics
Photon harvesting
Light engineering
Topological matter

ABSTRACT

Two-dimensional (2D) materials like transition metal dichalcogenides and Xenes are expected to bring exciting advancements in many fields of nanotechnology. The wealth of their electronic properties makes them appealing for a broad range of applications. In particular, in the framework of optics and photonics, three emerging routes where the key role of 2D materials will push forward the current state-of-the-art will be here outlined and discussed. Exerting control over the light-driven generation of spin-polarized dissipationless currents, enhancing the photon harvesting, and engineering the light-matter interaction are three challenges for 2D materials-based optics and photonics.

1. Introduction

The isolation of graphene by mechanical means set a milestone in condensed matter physics [1]. Today, graphene is no longer alone and a broad family of two-dimensional (2D) materials is currently the matter of investigation of many research groups around the world. Among the 2D materials, transition metal dichalcogenides (TMDs) and monoelemental graphene-like lattices, coined Xenes, are particularly attractive for their optical and photonic properties [2,3].

The booming interest in the Xenes started when the long-sought silicene was eventually synthesized on the Ag(111) surface using molecular beam epitaxy [4]. After that, going down along the IVA column of the periodic table, germanene, stanene, and plumbene were all found to exist being the closest relatives of graphene [2,5]. Surprisingly, out of the elements isoelectronic with carbon, the Xenes family expanded through the nearest columns, and hitherto we can list borophene and gallenene for the column IIIA, phosphorene, arsenene, antimonene, and bismuthene for the column VA, and finally selenene and tellurene for the column VIA [2,6]. The optical properties of the Xenes were initially investigated by theoretical methods, mostly on silicene, germanene, and stanene [7], and subsequently even experimentally by optical spectroscopy tools, including Raman [8–11] and ultrafast [12] spectroscopy as well as transmittance and reflectance measurements [13–16]. The wealth of the Xenes electronic properties is of course reflected in the broad range of applications where, for instance, plasmonics applications might be conceived using metallic Xenes, like borophene and gallenene [17], topological applications might exploit heavy Xenes, like stanene or bismuthene [5], and optoelectronics might be devised using semiconductive Xenes like selenene and tellurene [18,19].

In addition to Xenes, TMDs specialize their optoelectronic properties based on the details of the crystal structure with a key role played by the coordination environment of the transition metal and the occupancy of its *d*-orbital [20]. As a result, TMDs endowed with semiconductive to metallic character are available. Furthermore, for metal and chalcogen belonging to column VIB and A respectively, non-trivial band topology is expected when arranged in a distorted 1T′ crystal phase [21]. Notably, a thickness-dependent modification of the electronic band structure occurs thinning the bulk TMDs down to the monolayer limit [20]. In semiconductor monolayer TMDs, this modification is complemented by the indirect-to-direct transformation of the optical transitions along with the appearance of strong exciton effects, because of the reduced electrostatic screening potential, and valley degeneracy at the K and K' corners of the Brillouin zone because of the breaking of the inversion symmetry [22].

On the whole, the above-mentioned arguments make Xenes and TMDs appealing for photonic applications since they offer several

* Corresponding author.
** Corresponding author.
*** Corresponding author.
E-mail addresses: carlo.grazianetti@cnr.it (C. Grazianetti), christian.martella@cnr.it (C. Martella), eugenioluigi.cinquanta@cnr.it (E. Cinquanta).

https://doi.org/10.1016/j.omx.2021.100088
Received 28 July 2021; Received in revised form 27 August 2021; Accepted 31 August 2021
Available online 22 September 2021

options to meet the requirements of a variety of target functionalities.

Here, three emerging routes where TMDs and Xenes might constitute an advance for photonic applications will be outlined and corroborated by already reported findings in this framework. In the first one, we propose the exploitation of the topological state of matter in 2D for the realization of dissipationless optically controlled magnetic devices. In the second section, we will review how the optical properties of Xenes and TMDs change when compared to their bulk three-dimensional (3D) counterpart (if any) and how is possible to tune the absorption of light, and hence the light harvesting, in a broad range of the electromagnetic spectrum. Finally, in the third part, we discuss the impact on the light-matter interaction arising from the manipulation of the 2D materials at the nanoscale, including the effects related to strain engineering. Fig. 1 schematically resumes the three emerging routes described in detail in the next sections.

2. Section 1: optical control of the Quantum Spin Hall effect

The possible connection of topological insulators (TIs) and the 2D world appears as a promising option that could seed the rise of a dissipationless technology based on pure spin current. In some 2D materials, the non-trivial topological order gives rise to a new exotic state of matter known as the quantum spin Hall insulator (QSHI) state [23,24]. This exotic phase is a 2D bulk insulator with symmetry-protected conductive edge states lying in the bulk band gap and spatially located at the edges of the 2D lattice. Conductive states in QSHI are helical *i.e.*, up and down spins propagate in opposite directions along with one-dimensional (1D) ballistic transport channels that are robust against disorder, scattering, or any other TR-symmetry conserving excitation. This exotic effect was remarkably observed for the first time in HgTe/CdTe quantum wells through electrical measurements al cryogenic temperatures by M. König et al. [25]. To promote the QSH effect as a promising platform for the development of a new technological era, it is mandatory to develop a class of materials that harbor symmetry-protected dissipationless ballistic transport channels at room temperature. In this respect, honeycomb lattices made of heavy mass elements are needed to exploit the QSH effect at reasonable temperature because the spin-orbit coupling (SOC, a relativistic effect related to the atomic mass) converts the ideal Dirac semimetal into a QSHI state opening a bandgap. For example, SOC is so weak in graphene due to the light mass of carbon that the bandgap opening is negligible [26].

Recently, theory predicted different materials in the "flatland" as QSHI. In two independent works, X. Qian et al. and M. A. Cazalilla et al. proposed that monolayer TMDs in the 1T' phase should present the QSH effect at room temperature [27,28]. A pioneering experiment demonstrated that monolayer WTe_2 behaves as a QSHI at 100 K, hence boosting the research on the synthesis of new materials [29]. In this framework, artificial elemental 2D materials have been theoretically proposed as QSHIs with large bandgap [30–34]. Among them, stanene, the 2D honeycomb phase of tin, has been proposed as a QSHI when decorated with adatoms or mechanically deformed by the application of strain [35]. From a theoretical perspective, a more solid platform is stanene on α-Al_2O_3, which has been recently proposed as a room temperature QSHI without the need for any functionalization [36]. Experimentally, monoelemental Xenes have been recently synthesized on the Al_2O_3(0001) surface but no evidence of QSHI state have been reported yet [13,14]. These findings on silicene and stanene (discussed more in detail in the next section for different purposes) paved the way to the realization of heavy Xenes on transparent substrates at variance with the most relevant results achieved on the Xenes so far, mostly obtained on metallic substrates.

Leaving the group IVA road, in 2016 the epitaxial growth of a monolayer-thick bismuth film (bismuthene) with a large bandgap (ca. 800 meV) showing the QSH effect was demonstrated [37]. Fig. 2 shows the metallic edge states as observed through scanning tunneling spectroscopy (STS) (curves in Fig. 2a and maps in Fig. 2b, to be compared with topographical profile from the bulk to the edge in Fig. 2c).

To exploit topological effects in practical devices, the control of the physical properties is mandatory. For instance, established formalisms adopted for the description and prediction of fundamental effects in solids, such as optical transitions, could not hold anymore. In this respect, new selection rules governing electronic transition after photoexcitation are expected for 2D-TIs such quantum-well with zinc blende structures, given the broken inversion symmetry. For this class of materials, electron transitions from branches of the Dirac states with opposite spin (S), that violate the fundamental $\Delta S = 0$ selection rule, are possible and give rise to edge photocurrents controlled by radiation polarization through the circular photogalvanic effect [38,39].

Using light as the driver of new exotic phenomena hence emerges as a promising way to implement optically controlled devices. In this respect, the most intriguing properties of QSHI for potential applications are the helical edge states that host ballistic spin-polarized transport channels. The pure-spin ballistic current flowing at the edge states of QSHI will overcome the physical hurdles that hamper the exploitation of the electronic charge at the few nm technology node, such as energy dissipation and heating [40]. The on/off switch of these states with suitable light would allow for the realization of photonic topological devices. In this respect, the photo-spin-voltaic effect has been extensively exploited to generate an electric voltage from the pure spin current by shining light on magnetic materials/metals hybrid heterostructures [41]. This effect can be obtained also in non-magnetic materials, such as semiconductors coupled with metallic layer by exploiting circularly polarized light to generate two populations of spin-polarized electrons [42]. Remarkably, in QSHI, it is possible to obtain pure spin current with linearly polarized light and without the need for magnetic fields [43,44]. The possible exploitation of QSHI as light-controlled generators of pure spin current could lead to the realization of room-temperature spintronic devices with low energy dissipation. Among the Xenes, it is possible to envisage a bismuthene (stanene) sample prepared with the Dirac states unoccupied by moving the Fermi level in the bulk trivial valence band maximum with an electrostatic gating. Then, the two helical branches of the Dirac states can be populated by excitation with linearly polarized photons. To avoid the population of trivial states in the conduction band, photons with E_{ph}<600 meV (300 meV, for stanene) *i.e.*, mid-IR light, must be used, as depicted in Fig. 2d. A pure-spin current will hence start to flow in the dissipationless symmetry-protected edge states but neither net charge current nor net magnetization will be present in the system. This

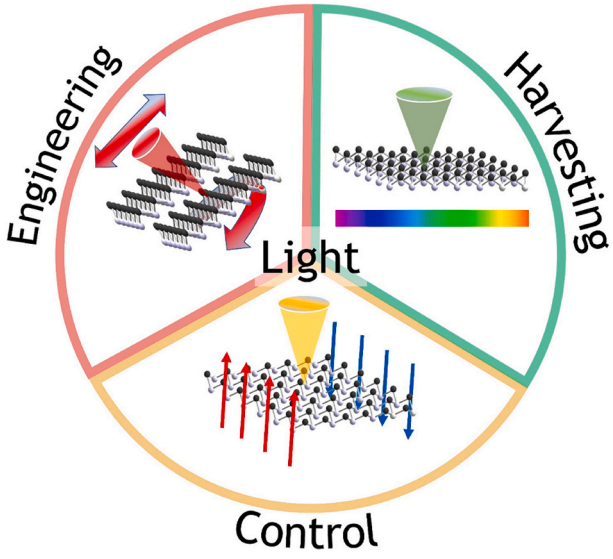

Fig. 1. Emerging routes where 2D materials might constitute advances in photonic applications.

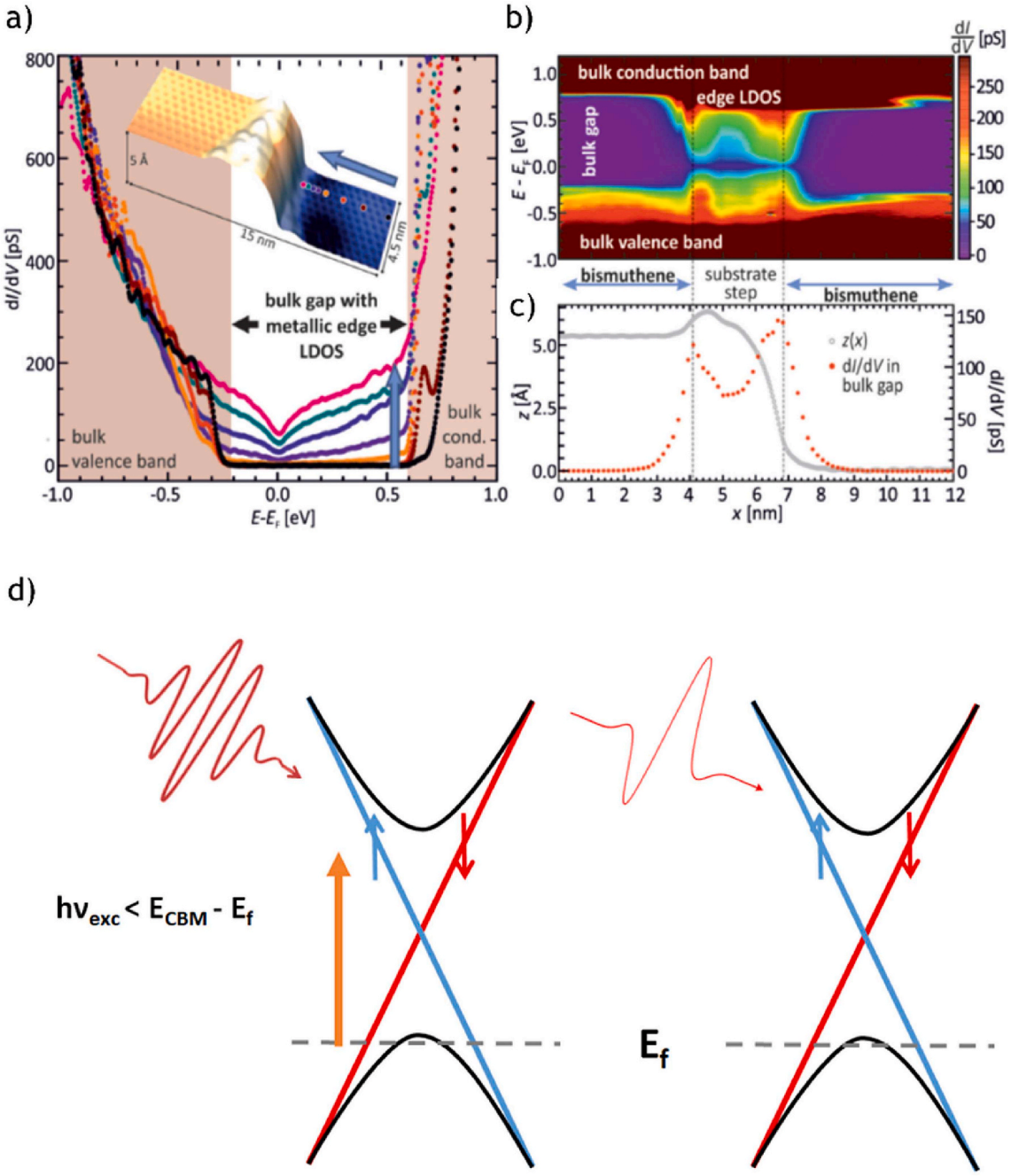

Fig. 2. a) STS spectra of bismuthene showing the ~0.8 eV bandgap and metallic-like edges. b) STS map evidencing the localization of metallic states at the edges. c) Step profile of bismuthene on SiC (left scale) compare with the dI/dV signal along the step (right scale). Adapted with permission from Ref. [37]. d) Linear polarized mid-IR beam will excite carriers from the bulk valence band to Dirac edge states (left), then a pure spin current will start to flow at the sample edges (right).

all-optical switching of a pure spin current can be then exploited for instance as a spin injector in optical-spintronic devices like spin valves, magnetic tunnel junctions, and all spin logic devices with the advantages of the topological character of the exploited transport channel.

3. Section 2: photon harvesting by tuning the optical absorption

In addition to the topological properties discussed above, 2D materials like Xenes and TMDs show intriguing absorption spectra in a broad electromagnetic range, thus envisioning new routes in photon harvesting. Most importantly, the 2D materials absorption spectra look very different from the 3D bulk counterparts, hence their advantages are the scaling of the device dimensions and the broadening of the accessible electromagnetic spectrum. The graphene absorption spectrum is characterized by a constant absorption value equal to $\pi\alpha$ (where $\alpha = e^2/\hbar c$ is the fine structure constant) in a broad range of the photon energies and absorption rises only in the UV range due to the π-π^* transition related to a van Hove singularity in the joint density of states (JDOS) [45,46]. On the one hand, it is quite surprising that post-graphene Xenes like silicene and germanene keep a similar absorption spectrum despite their buckled lattice and are featured by a constant absorption at low frequencies and characteristic absorption peaks at higher frequencies related to interband transitions [46]. On the other hand, the different JDOS give rise to different absorption spectra in the same photon range (typically from THz to UV) where the original transparency carried by graphene is progressively lost in silicene, germanene, and stanene by absorption

features (typically the π-π* transition occurs at lower photon energies than in graphene) [46]. The urgent need to find alternative solutions to silicon for photonic applications might be silicon itself when scaled down to 2D. Most silicon nanotechnologies, especially in the electronics field, rely on bulk silicon and recently many efforts were devoted to merge electronic and photonics systems on a chip [47]. In this framework, the recent outcomes on the silicon growth on a transparent substrate like Al_2O_3(0001) enabled to unravel different optical propertiess in the silicon thickness range between 0.5 and 7 nm (see inset of Fig. 3a) [13]. At the 2D limit *i.e.*, 0.5 nm, silicene endowed with graphene-like properties, namely the evidence of the Dirac electrodynamics is fully singled out according to the theoretical model, are disclosed with slight modifications induced by the supporting template. Indeed, the degree of interaction between silicene and Al_2O_3(0001) turns out to induce small energy shifts in the interband transitions when compared to the free-standing silicene (interestingly, the σ-σ* transition is more affected than the π-π* transition). Nevertheless, the observed experimental optical properties are fully consistent with the theoretical prediction of a weakly interacting silicene [13]. Increasing the silicon thickness, the optical properties of silicene progressively disappear (even if the spectrum is always reminiscent of the Dirac-like behavior) and show a new trend characterized by an enhanced absorption below the bandgap of both amorphous and crystalline bulk silicon as reported in Fig. 3a. More intriguingly, the absorption spectra of silicon grown on Al_2O_3(0001) differ also from those of theoretically modeled silicon allotropes like silicite [48–50]. If properly engineered these thin silicon films might pave the way to the absorption below the mid-IR thus extending the range of photon energy available for silicon-based photonic devices. Interestingly, the same substrate Al_2O_3(0001) can host even stanene-like nanosheets therein showing absorption spectra with freestanding stanene features (see Fig. 3b) [46,51], but, most importantly, with an overall behavior in the THz-UV different from tin oxides or conventional metallic tin phases [14]. Therefore, it is possible to figure out specific photonic applications based on the artificial synthesis of Xenes beyond graphene on a transparent substrate like Al_2O_3(0001) thus aiming at the development of photon harvesting in the region of the electromagnetic spectrum not considered in their bulk counterparts. In this respect, further advancement will rely on the integration with the existing silicon technology as recently proposed for vis-NIR photodetectors coupling 2D bismuth with silicon [52]. Even if well-known and studied in their bulk form, elements like silicon, germanium, or bismuth surprisingly show new optical properties when scaled down to the 2D regime. If the optical properties of the Xenes have been disclosed only recently, their knowledge on TMDs is today more advanced.

Indeed, TMDs endowed with a semiconductor character are also promising candidates for nanophotonics applications, in particular when a tunable optical absorption response is required. Semiconductor TMDs, like MoS_2, show unique optical properties, which stem from the indirect-to-direct transition of the bandgap varying their thickness from the bulk down to the monolayer limit [20,22]. Combined with the broad

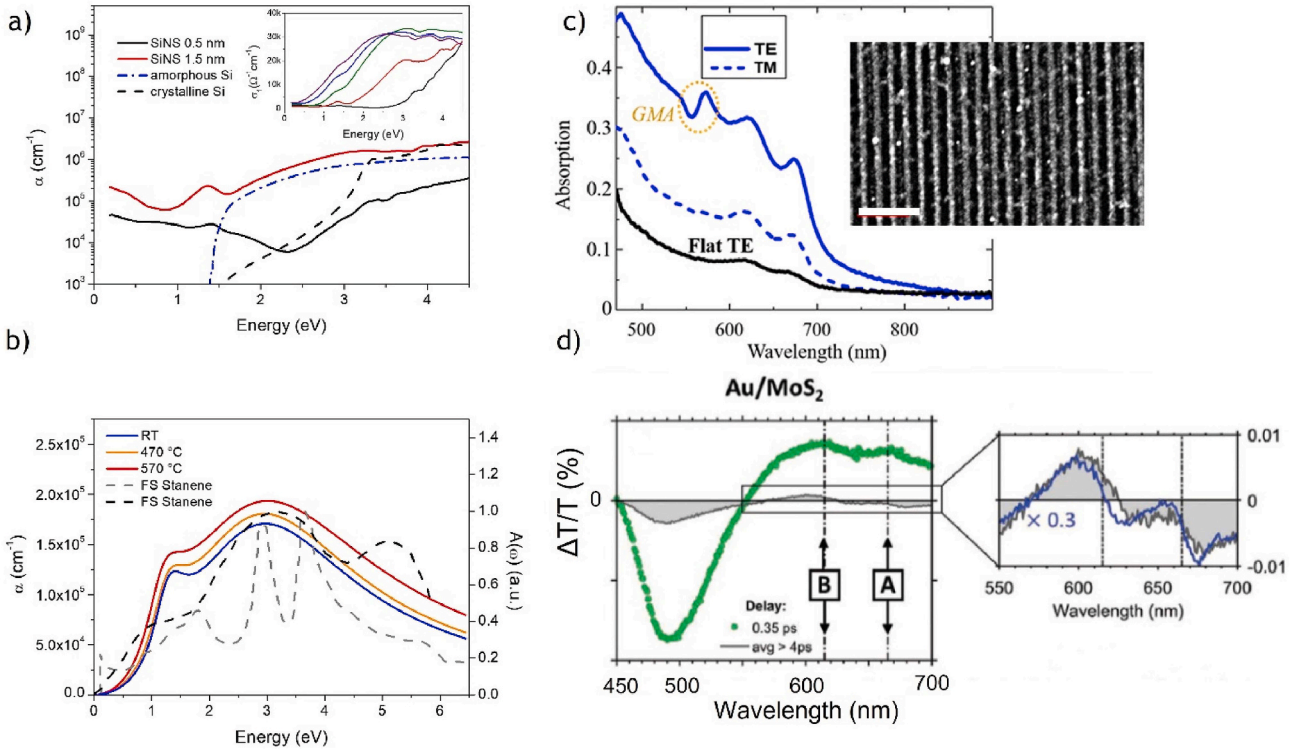

Fig. 3. (a) Absorption coefficients α(ω) of 0.5 (black) and 1.5 (red) nm-thick silicon nanosheets on Al_2O_3(0001) compared with amorphous (blue dash-dotted) and crystalline (black dashed) bulk silicon showing extended absorption below the bandgap. The inset shows the optical conductivity for 0.5 (black), 1.5 (red), 3 (green), 5 (blue), and 7 (purple) nm-thick silicon nanosheets evidencing the thickness-dependent behavior of their optical response from IR to UV. Adapted with permission from Ref. [13]. (b) Absorption coefficients α(ω) (left scale) of 0.5 nm-thick tin nanosheets grown on Al_2O_3(0001) at different substrate temperatures: RT (blue), 470 °C (orange), and 570 °C (red), compared with two different theoretical absorbances (right scale) of freestanding stanene from Ref. [46] (dashed gray) and from Ref. [51] (dashed black). Adapted with permission from Ref. [14]. (c) Optical absorption spectra of MoS_2 nanostripe array, see scanning electron microscopy image in the inset with scale bar 1 μm, for polarization of the illumination beam with the electric field oriented parallel (TE) and perpendicular (TM) with respect to the major axis of the nanostripes (continuous and dashed blue line, respectively), see also inset in Fig. 4a. The excitation of GMA resonances is confirmed by local minima in the absorption spectra characterized by a spatial period-dependent dispersion relation. The absorption spectra of a reference flat MoS_2 sample are also shown for comparison (black line). Adapted with permission from Ref. [62] (d) Ultrafast transient absorption spectra of a hybrid nanosystem constituted by rippled MoS_2 layers decorated with plasmonic gold nanostripes. The relative differential transmittance (ΔT/T) shows photo-bleaching and photoinduced absorption spectral features because of the charge transfer between the plasmonic excitation into the nanostripes and the TMDs excitonic resonances (A, B excitons). Adapted with permission from Ref. [65]. (For interpretation of the references to colour in this figure legend, the reader is referred to the Web version of this article.)

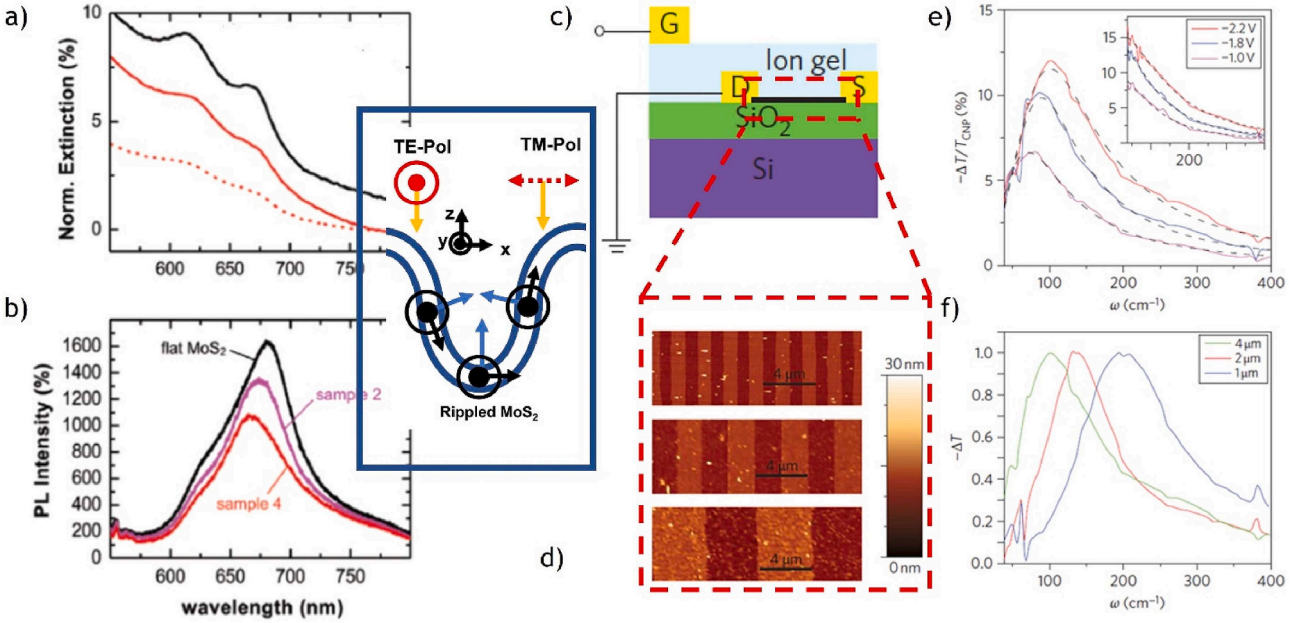

Fig. 4. a) Experimental extinction spectra in the spectral region of the A and B exciton resonances of rippled MoS_2 layers for TE and TM polarization of the incident light (red straight and dashed line, respectively). The spectrum of reference flat MoS_2 layers is shown for comparison (black line). The inset shows the experimental configuration of the optical measurements and the adopted theoretical model to demonstrate that the dichroism, observed in the extinction spectra, stems from the morphological conformal orientation of the permittivity tensor (in-plane/out-of-plane component in black/blue arrows). b) In the rippled MoS_2 layers of the panel (a), changes into the permittivity tensor due to strain are responsible for spectral shift and intensity reduction in the PL emission. Adapted with permissions from Ref. [75]. c) Sketch of the device incorporating the graphene micro-ribbon array on a Si/SiO_2 substrate and covered by an ion gel. d) AFM images of three different micro-ribbons with widths of 1 (top), 2 (middle) and 4 (bottom) μm. e) Control of terahertz resonance of plasmon excitations through electrical gating when the incident radiation is polarized perpendicular to the micro-ribbons. The inset shows corresponding spectra due to free carrier absorption for incident radiation polarized parallel to the ribbons. f) Control of plasmon excitations frequency with different graphene micro-ribbon widths for the same doping concentration (1.5×10^{13} cm^{-2}). The plasmon resonance frequency shifts from 3 to 6 THz when micro-ribbon width decreases from 4 to 1 μm. Adapted with permission from Ref. [77]. (For interpretation of the references to colour in this figure legend, the reader is referred to the Web version of this article.)

spectral range of the bandgap (from visible to near IR), these optical features pave the way not only to photon harvesting for sensing or detection applications [53,54], but also for energy conversions like in photovoltaics and photocatalysis [55–59]. Nevertheless, some limitations must be addressed given 2D TMDs technological exploitation as optical absorber materials. The main one is the out-of-plane reduced dimensionality, *i.e.* their thickness, which hinders the effective absorption of light limiting the optical path to a subwavelength length scale.

Effectively coupling of light with the TMDs is achieved by adopting photon harvesting strategies. Anticipating some arguments of the next section, these strategies consist in TMDs engineering at the nanoscale and/or in the realization of hybrid heterostructures combining, for example, plasmonic nanosystem with 2D materials [60]. The flat-optics approach takes advantage of the light scattering and near-field confinement properties of subwavelength lattices to tailor the light-matter interaction at the 2D level [61]. Modelling MoS_2 nanosheets in the shape of subwavelength 1D nanostripe array leads to light confinement through excitation of guided mode anomalies (GMA) at the interfaces of the 2D material and its supporting substrate [62,63]. The GMA resonances, tunable over the visible to near IR range, enables to amplify the optical absorption of the 1D MoS_2 array of a relative 400% compared to flat reference nanosheets. This extraordinary amplification of the optical absorption is observed in correspondence of the TMD exciton spectral frequencies as a function of the normal incidence light polarization, namely for the electric field oriented parallel (TE polarization) and perpendicular (TM polarization) with respect to the major axis of the nanostripes, see Fig. 3c [62,63]. As mentioned above, the alternative photon harvesting scheme consists of the coupling between plasmons and 2D material semiconductors. In such a hybrid heterostructure, the injection of extra charge carriers into the semiconductor is mediated by the generation of plasmonic resonances into noble metal nanostructures. More in detail, the intrinsic low light absorption in the 2D material is enhanced by the collection of a non-thermalized population of high energy electrons (hot-electrons) generated into the plasmonic medium as revealed by ultrafast transient absorption spectroscopy. Matching the transient optical response of the pristine MoS_2 layers [64] with that of the hybrid heterostructure provides compelling evidence that the hot-electrons population is effectively transferred into the TMD (see Fig. 3d), otherwise it would thermalize by electron-phonon scattering events on a few picoseconds time scale in the absence of the TMD acceptor [65].

4. Section 3: light engineering

Many exciting scenarios develop when considering 2D semiconductor TMDs as a platform for harnessing and manipulating light. Tentatively the results described below could be potentially extended also to semiconductive Xenes, even if no experimental results have been reported yet to our knowledge. Attempts at generating deterministic sources of single-photon emission consist in artificially inducing quantum confinement potentials in 2D TMDs thus driving radiative exciton recombination. The built-in potentials are typically the results of the introduction of morphological modifications or defects into the nanosheets [66]. Indeed, shaping the layers into arbitrary curved paths represents a knob for tailoring the electronic bandstructure of the TMDs by deterministic strain engineering [67]. Notably, the potential to electrically trigger the emission points to the development of innovative functional devices, like quantum light-emitting diodes, aiming at the realization of integrated on-chip quantum technologies [68]. In this respect, quantum communication and cryptography are only two of the envisaged applications where the realization of deterministic single-photon sources may have a pivotal role [69]. However, TMDs

engineering promises not only technological advances in the development of quantum photon sources. Progresses towards the realization of TMDs-based optical metasurfaces consist of both the nanoscale patterning of the 2D material on the subwavelength scale and the coupling with metal-dielectric photonic structures [60,61]. In this context, the possibility to effectively implement optical phase shifts, coherent light scattering, and polarization state control at the atomic thickness level would open the door to the realization of ultrathin flat lenses, holograms, mirrors, and so on with potential novel functional integration into optoelectronic circuits [70–72]. Interestingly, apart from the linear and nonlinear optical properties, TMDs-based optical metasurfaces can take advantage of the spin and valley degree of freedom. The breaking of the crystal inversion symmetry, in hexagonal monolayer TMD semiconductor, combined with TR symmetry and SOC leads to inequivalent K and K' valleys at the corners of the Brillouin zone [22]. As a result, under circularly polarized light, the TMD acquires different exciton populations corresponding to the inequivalent valleys [73]. Recently, to overcome the fast valley depolarization of the population, a hybrid all-dielectric combination of the monolayer TMD with a defective photonic crystal has been proposed [74]. At variance with the pristine monolayer, the photoluminescence (PL) emission of the hybrid system shows a spin–split dispersion from valley excitons in momentum space, manifesting as the photonic Rashba effect [74]. Further approaches to enable light control are based on the exploitation of the intrinsic anisotropy of the nanosheets as a knob to spatially modulate the optical response [75]. For instance, a giant linear optical dichroism at normal incidence has been observed in nanoscale rippled MoS_2 layers in correspondence of the exciton spectral frequencies [75]. The in-depth analysis of the observed dichroism, supported by full-vectorial numerical simulations, reveals a strong correlation with the nanoscale curvature and slope control of the nanosheets. Intriguingly, the material engineering of the 2D nanosheets, obtained by tailoring their intrinsic anisotropy at the nanoscale, reflects into an anisotropic permittivity tensor and giant optical extinction when the incident electric field is orthogonal to the long axis of the rippled nanostructures (TM polarization), see Fig. 4a. Moreover, a secondary effect of geometrically induced strain is responsible for the modification observed into the PL emission of the nanosheets, see Fig. 4b [75]. A similar material engineering approach can be devised for the Xenes, although the targeted applications seem today to be limited to a more restricted field in comparison with those of TMDs.

Xenes provided with Dirac electrodynamics can be inserted into metamaterials for exploring and tuning their plasmonic response in the mid-IR and THz regions of the electromagnetic spectrum. Plasmons are quantized collective oscillations of electrons that can be exploited in optoelectronics, nonlinear optics, optical sensing, photovoltaic, and medical diagnostics. Engineered graphene and topological insulators (like Bi_2Se_3) microribbon arrays have been already fabricated thus proving that plasmon resonances can be tuned over a broad range of THz frequency range by optimizing geometrical parameters like the ribbon width or by electrostatic doping [76,77]. Quite similarly, recently the same approach has been used for THz third-harmonic generation in a graphene-based metamaterial [78]. In this framework, just considering the Xenes among the so-called THz materials, *i.e.* materials enabling to access the THz region for telecommunication or medicine applications, specific platforms should be developed accordingly [79]. Fig. 4c shows the realization of a device scheme where a metasurface with a subwavelength grating (to provide extra-momentum necessary for plasmon excitation) is obtained by patterning the graphene surface as reported in the atomic force microscopy (AFM) image of Fig. 4d [77]. Such ribbon arrays enabled to tune both resonance intensity (Fig. 4e) and frequency (Fig. 4f) through ion liquid electric gating and ribbon width, respectively. Plasmonic gratings like that illustrated for graphene can be straightforwardly extended to other Dirac Xenes like silicene, germanene, and stanene, where the SOC effect makes them appealing from the topological point of view. In this framework, the configuration where the Xene is encapsulated in between optically transparent layers (like that mentioned above for silicene and stanene [13,14]) can be used to access the topological plasmonic resonance of Dirac electrons even in these post-graphene materials or aiming at expanding the degree of control over the frequency range and resonance intensity of the plasmons.

5. Conclusions

In summary, three emerging routes where 2D materials like Xenes and TMDs are expected to bring advancements in the fields of photonics have been presented. Further efforts are needed in the growing methods and integration processes enabling the exploitation of the properties of the 2D materials. Indeed, large-scale growth on optically compatible substrates can be effectively achieved for TMDs (where the main issue is reproducibility), whereas for Xenes this is an urgent task which requires to face challenges concerning their intrinsic artificial nature (such as the need of specific lattice-matched supporting substrates) and stabilization issues (such as the need of encapsulation strategies preventing degradation in ambient conditions). By and large, the three routes discussed here span many aspects of photonics including topological matter, photon harvesting, and light engineering, therein looking promising for many exciting outcomes shortly.

CRediT authorship contribution statement

C. Grazianetti: Conceptualization, Writing – original draft, Preparation, Writing – review &; editing. **C. Martella:** Conceptualization, Writing – original draft, Preparation, Writing – review &; editing. **E. Cinquanta:** Conceptualization, Writing – review &; editing, All authors approved the final version of the manuscript.

Declaration of competing interest

The authors declare that they have no known competing financial interests or personal relationships that could have appeared to influence the work reported in this paper.

Acknowledgment

E.C. acknowledges financial support from MIUR PRIN aSTAR, Grant No. 2017RKWTMY and from the European Union's Horizon 2020 research and innovation programme through the MSCA-ITN SMART-X (GA 860553).

References

[1] A.C. Ferrari, F. Bonaccorso, V. Fal'ko, K.S. Novoselov, S. Roche, P. Bøggild, S. Borini, F.H.L. Koppens, V. Palermo, N. Pugno, J.A. Garrido, R. Sordan, A. Bianco, L. Ballerini, M. Prato, E. Lidorikis, J. Kivioja, C. Marinelli, T. Ryhänen, A. Morpurgo, J.N. Coleman, V. Nicolosi, L. Colombo, A. Fert, M. Garcia-Hernandez, A. Bachtold, G.F. Schneider, F. Guinea, C. Dekker, M. Barbone, Z. Sun, C. Galiotis, A.N. Grigorenko, G. Konstantatos, A. Kis, M. Katsnelson, L. Vandersypen, A. Loiseau, V. Morandi, D. Neumaier, E. Treossi, V. Pellegrini, M. Polini, A. Tredicucci, G.M. Williams, B. Hee Hong, J.-H. Ahn, J. Min Kim, H. Zirath, B. J. van Wees, H. van der Zant, L. Occhipinti, A. Di Matteo, I.A. Kinloch, T. Seyller, E. Quesnel, X. Feng, K. Teo, N. Rupesinghe, P. Hakonen, S.R.T. Neil, Q. Tannock, T. Löfwander, J. Kinaret, Science and technology roadmap for graphene, related two-dimensional crystals, and hybrid systems, Nanoscale 7 (2015) 4598–4810, https://doi.org/10.1039/C4NR01600A.

[2] C. Grazianetti, C. Martella, A. Molle, The Xenes generations: a taxonomy of epitaxial single-element 2D materials, Phys. Status Solidi Rapid Res. Lett. 14 (2020), 1900439, https://doi.org/10.1002/pssr.201900439.

[3] S. Manzeli, D. Ovchinnikov, D. Pasquier, O.V. Yazyev, A. Kis, 2D transition metal dichalcogenides, Nat. Rev. Mater. 2 (2017) 1–15, https://doi.org/10.1038/natrevmats.2017.33.

[4] P. Vogt, P. De Padova, C. Quaresima, J. Avila, E. Frantzeskakis, M.C. Asensio, A. Resta, B. Ealet, G. Le Lay, Silicene: compelling experimental evidence for graphenelike two-dimensional silicon, Phys. Rev. Lett. 108 (2012), 155501, https://doi.org/10.1103/PhysRevLett.108.155501.

[5] A. Zhao, B. Wang, Two-dimensional graphene-like Xenes as potential topological materials, Apl. Mater. 8 (2020) 30701, https://doi.org/10.1063/1.5135984.

[6] N.R. Glavin, R. Rao, V. Varshney, E. Bianco, A. Apte, A. Roy, E. Ringe, P.M. Ajayan, Emerging applications of elemental 2D materials, Adv. Mater. 32 (2020) 1904302, https://doi.org/10.1002/adma.201904302.

[7] F. Bechstedt, L. Matthes, P. Gori, O. Pulci, Optical properties of silicene and related materials from first principles. https://doi.org/10.1007/978-3-319-99964-7_4, 2018, 73-98.

[8] E. Cinquanta, E. Scalise, D. Chiappe, C. Grazianetti, B. Van Den, Getting through the nature of silicene : sp 2 -sp 3 two- dimensional silicon nanosheet, J. Phys. Chem. C (2013) 1–24, https://doi.org/10.1021/jp405642g.

[9] S. Sheng, J.-B. Wu, X. Cong, Q. Zhong, W. Li, W. Hu, J. Gou, P. Cheng, P.-H. Tan, L. Chen, K. Wu, Raman spectroscopy of two-dimensional borophene sheets, ACS Nano 13 (2019) 4133–4139, https://doi.org/10.1021/acsnano.8b08909.

[10] Y. Du, G. Qiu, Y. Wang, M. Si, X. Xu, W. Wu, P.D. Ye, One-dimensional van der Waals material tellurium: Raman spectroscopy under strain and magneto-transport, Nano Lett. 17 (2017) 3965–3973, https://doi.org/10.1021/acs.nanolett.7b01717.

[11] J. Zhuang, N. Gao, Z. Li, X. Xu, J. Wang, J. Zhao, S.X. Dou, Y. Du, Cooperative electron–phonon coupling and buckled structure in germanene on Au(111), ACS Nano 11 (2017) 3553–3559, https://doi.org/10.1021/acsnano.7b00687.

[12] E. Cinquanta, G. Fratesi, S. dal Conte, C. Grazianetti, F. Scotognella, S. Stagira, C. Vozzi, G. Onida, A. Molle, Optical response and ultrafast carrier dynamics of the silicene-silver interface, Phys. Rev. B 92 (2015), 165427, https://doi.org/10.1103/PhysRevB.92.165427.

[13] C. Grazianetti, S. De Rosa, C. Martella, P. Targa, D. Codegoni, P. Gori, O. Pulci, A. Molle, S. Lupi, Optical conductivity of two-dimensional silicon: evidence of Dirac electrodynamics, Nano Lett. 18 (2018) 7124–7132, https://doi.org/10.1021/acs.nanolett.8b03169.

[14] C. Grazianetti, E. Bonaventura, C. Martella, A. Molle, S. Lupi, Optical properties of stanene-like nanosheets on Al 2 O 3 (0001): implications for Xene photonics, ACS Appl. Nano Mater. 4 (2021) 2351–2356, https://doi.org/10.1021/acsanm.0c03221.

[15] J. Genser, D. Nazzari, V. Ritter, O. Bethge, K. Watanabe, T. Taniguchi, E. Bertagnolli, F. Bechstedt, A. Lugstein, Optical signatures of Dirac electrodynamics for hBN-passivated silicene on Au(111), Nano Lett. (2021), https://doi.org/10.1021/acs.nanolett.1c01440 acs.nanolett.1c01440.

[16] C. Hogan, O. Pulci, P. Gori, F. Bechstedt, D.S. Martin, E.E. Barritt, A. Curcella, G. Prevot, Y. Borensztein, Optical properties of silicene, Si/Ag(111), and Si/Ag (110), Phys. Rev. B 97 (2018), 195407, https://doi.org/10.1103/PhysRevB.97.195407.

[17] C. Lian, S.-Q. Hu, J. Zhang, C. Cheng, Z. Yuan, S. Gao, S. Meng, Integrated plasmonics: broadband Dirac plasmons in borophene, Phys. Rev. Lett. 125 (2020), 116802, https://doi.org/10.1103/PhysRevLett.125.116802.

[18] J. Qin, G. Qiu, J. Jian, H. Zhou, L. Yang, A. Charnas, D.Y. Zemlyanov, C.Y. Xu, X. Xu, W. Wu, H. Wang, P.D. Ye, Controlled growth of a large-size 2D selenium nanosheet and its electronic and optoelectronic applications, ACS Nano 11 (2017) 10222–10229, https://doi.org/10.1021/acsnano.7b04786.

[19] C. Shen, Y. Liu, J. Wu, C. Xu, D. Cui, Z. Li, Q. Liu, Y. Li, Y. Wang, X. Cao, H. Kumazoe, F. Shimojo, A. Krishnamoorthy, R.K. Kalia, A. Nakano, P.D. Vashishta, M.R. Amer, A.N. Abbas, H. Wang, W. Wu, C. Zhou, Tellurene photodetector with high gain and wide bandwidth, ACS Nano 14 (2020) 303–310, https://doi.org/10.1021/acsnano.9b04507.

[20] M. Chhowalla, H.S. Shin, G. Eda, L.-J. Li, K.P. Loh, H. Zhang, The chemistry of two-dimensional layered transition metal dichalcogenide nanosheets, Nat. Chem. 5 (2013) 263–275, https://doi.org/10.1038/nchem.1589.

[21] D.-H. Choe, H.-J. Sung, K.J. Chang, Understanding topological phase transition in monolayer transition metal dichalcogenides, Phys. Rev. B 93 (2016), 125109, https://doi.org/10.1103/PhysRevB.93.125109.

[22] K.F. Mak, J. Shan, Photonics and optoelectronics of 2D semiconductor transition metal dichalcogenides, Nat. Photonics 10 (2016) 216–226, https://doi.org/10.1038/nphoton.2015.282.

[23] F.D.M. Haldane, Model for a quantum Hall effect without landau levels: condensed-matter realization of the "parity anomaly, Phys. Rev. Lett. 61 (1988) 2015–2018, https://doi.org/10.1103/PhysRevLett.61.2015.

[24] B.A. Bernevig, S.-C. Zhang, Quantum spin Hall effect, Phys. Rev. Lett. 96 (2006), 106802, https://doi.org/10.1103/PhysRevLett.96.106802.

[25] M. König, S. Wiedmann, C. Brüne, A. Roth, H. Buhmann, L.W. Molenkamp, X.-L. Qi, S.-C. Zhang, Quantum spin Hall insulator state in HgTe quantum wells, Science (80-.) 318 (2007) 766–770, https://doi.org/10.1126/SCIENCE.1148047.

[26] C.L. Kane, E.J. Mele, Quantum spin Hall effect in graphene, Phys. Rev. Lett. 95 (2005), 226801, https://doi.org/10.1103/PhysRevLett.95.226801.

[27] X. Qian, J. Liu, L. Fu, J. Li, Quantum spin Hall effect in two-dimensional transition metal dichalcogenides, Science (80-.) 346 (2014) 1344–1347, https://doi.org/10.1126/science.1256815.

[28] M.A. Cazalilla, H. Ochoa, F. Guinea, Quantum spin Hall effect in two-dimensional crystals of transition-metal dichalcogenides, Phys. Rev. Lett. 113 (2014), 077201, https://doi.org/10.1103/PhysRevLett.113.077201.

[29] S. Wu, V. Fatemi, Q.D. Gibson, K. Watanabe, T. Taniguchi, R.J. Cava, P. Jarillo-Herrero, Observation of the quantum spin Hall effect up to 100 kelvin in a monolayer crystal, Science (80-.) 359 (2018) 76–79, https://doi.org/10.1126/science.aan6003.

[30] W. Luo, H. Xiang, Room temperature quantum spin Hall insulators with a buckled square lattice, Nano Lett. 15 (2015) 3230–3235, https://doi.org/10.1021/acs.nanolett.5b00418.

[31] R. Zhang, C. Zhang, W. Ji, P. Li, P. Wang, S. Li, S. Yan, Silicon-based chalcogenide: unexpected quantum spin Hall insulator with sizable band gap, Appl. Phys. Lett. 109 (2016), 182109, https://doi.org/10.1063/1.4966124.

[32] H. Zhao, C. Zhang, W. Ji, R. Zhang, S. Li, S. Yan, B. Zhang, P. Li, P. Wang, Unexpected giant-gap quantum spin Hall insulator in chemically decorated plumbene monolayer, Sci. Rep. 6 (2016), 20152, https://doi.org/10.1038/srep20152.

[33] I.A. Nechaev, S.V. Eremeev, E.E. Krasovskii, P.M. Echenique, E.V. Chulkov, Quantum spin Hall insulators in centrosymmetric thin films composed from topologically trivial BiTeI trilayers, Sci. Rep. 7 (2017) 43666, https://doi.org/10.1038/srep43666.

[34] X. Wang, P. Li, Z. Ran, W. Luo, Quantum spin Hall insulators in chemically functionalized as (110) and Sb (110) films, Chin. Phys. B 27 (2018), 087305, https://doi.org/10.1088/1674-1056/27/8/087305.

[35] Y. Xu, B. Yan, H.-J. Zhang, J. Wang, G. Xu, P. Tang, W. Duan, S.-C. Zhang, Large-gap quantum spin Hall insulators in tin films, Phys. Rev. Lett. 111 (2013), 136804, https://doi.org/10.1103/PhysRevLett.111.136804.

[36] H. Wang, S.T. Pi, J. Kim, Z. Wang, H.H. Fu, R.Q. Wu, Possibility of realizing quantum spin Hall effect at room temperature in stanene/Al2O3(0001), Phys. Rev. B 94 (2016), 035112, https://doi.org/10.1103/PhysRevB.94.035112.

[37] F. Reis, G. Li, L. Dudy, M. Bauernfeind, S. Glass, W. Hanke, R. Thomale, J. Schäfer, R. Claessen, Bismuthene on a SiC substrate: a candidate for a high-temperature quantum spin Hall material, Science 357 (2017) 287–290, https://doi.org/10.1126/science.aai8142.

[38] M. V Durnev, S.A. Tarasenko, Optical properties of helical edge channels in zinc-blende-type topological insulators: selection rules, circular and linear dichroism, circular and linear photocurrents, J. Phys. Condens. Matter 31 (2019), 035301, https://doi.org/10.1088/1361-648X/aaf024.

[39] X. Zhang, W.-Y. Shan, D. Xiao, Optical selection rule of excitons in gapped chiral fermion systems, Phys. Rev. Lett. 120 (2018), 077401, https://doi.org/10.1103/PhysRevLett.120.077401.

[40] S. Salahuddin, K. Ni, S. Datta, The era of hyper-scaling in electronics, Nat. Electron. 1 (2018) 442–450, https://doi.org/10.1038/s41928-018-0117-x.

[41] D. Ellsworth, L. Lu, J. Lan, H. Chang, P. Li, Z. Wang, J. Hu, B. Johnson, Y. Bian, J. Xiao, R. Wu, M. Wu, Photo-spin-voltaic effect, Nat. Phys. 12 (2016) 861–866, https://doi.org/10.1038/nphys3738.

[42] F. Bottegoni, M. Celebrano, M. Bollani, P. Biagioni, G. Isella, F. Ciccacci, M. Finazzi, Spin voltage generation through optical excitation of complementary spin populations, Nat. Mater. 13 (2014) 790–795, https://doi.org/10.1038/nmat4015.

[43] J. Wang, B.-F. Zhu, R.-B. Liu, Proposal for direct measurement of a pure spin current by a polarized light beam, Phys. Rev. Lett. 100 (2008), 086603, https://doi.org/10.1103/PhysRevLett.100.086603.

[44] J. Wang, S.-N. Ji, B.-F. Zhu, R.-B. Liu, Optical effects of spin currents in semiconductors, Phys. Rev. B 86 (2012), 045215, https://doi.org/10.1103/PhysRevB.86.045215.

[45] R.R. Nair, P. Blake, A.N. Grigorenko, K.S. Novoselov, T.J. Booth, T. Stauber, N.M. R. Peres, A.K. Geim, Fine structure constant defines visual transparency of graphene, Science (80-.) 320 (2008), https://doi.org/10.1126/SCIENCE.1156965, 1308–1308.

[46] L. Matthes, O. Pulci, F. Bechstedt, Optical properties of two-dimensional honeycomb crystals graphene, silicene, germanene, and tinene from first principles, New J. Phys. 16 (2014), 105007, https://doi.org/10.1088/1367-2630/16/10/105007.

[47] A.H. Atabaki, S. Moazeni, F. Pavanello, H. Gevorgyan, J. Notaros, L. Alloatti, M. T. Wade, C. Sun, S.A. Kruger, H. Meng, K. Al Qubaisi, I. Wang, B. Zhang, A. Khilo, C.V. Baiocco, M.A. Popović, V.M. Stojanović, R.J. Ram, Integrating photonics with silicon nanoelectronics for the next generation of systems on a chip, Nature 556 (2018) 349–354, https://doi.org/10.1038/s41586-018-0028-z.

[48] S. Botti, J.A. Flores-Livas, M. Amsler, S. Goedecker, M.A.L. Marques, Low-energy silicon allotropes with strong absorption in the visible for photovoltaic applications, Phys. Rev. B Condens. Matter 86 (2012), 121204, https://doi.org/10.1103/PhysRevB.86.121204.

[49] D.Y. Kim, S. Stefanoski, O.O. Kurakevych, T.A. Strobel, Synthesis of an open-framework allotrope of silicon, Nat. Mater. 14 (2014) 169–173, https://doi.org/10.1038/nmat4140.

[50] S. Cahangirov, V.O. Özçelik, A. Rubio, S. Ciraci, Silicite: the layered allotrope of silicon, Phys. Rev. B 90 (2014), 085426, https://doi.org/10.1103/PhysRevB.90.085426.

[51] R. John, B. Merlin, Optical properties of graphene, silicene, germanene, and stanene from IR to far UV – a first principles study, J. Phys. Chem. Solid. 110 (2017) 307–315, https://doi.org/10.1016/j.jpcs.2017.06.026.

[52] Z. Dang, W. Wang, J. Chen, E.S. Walker, S.R. Bank, D. Akinwande, Z. Ni, L. Tao, Vis-NIR photodetector with microsecond response enabled by 2D bismuth/Si(111) heterojunction, 2D Mater. 8 (2021), 035002, https://doi.org/10.1088/2053-1583/abea65.

[53] C. Xie, C. Mak, X. Tao, F. Yan, Photodetectors based on two-dimensional layered materials beyond graphene, Adv. Funct. Mater. 27 (2017), 1603886, https://doi.org/10.1002/adfm.201603886.

[54] F.H.L. Koppens, T. Mueller, P. Avouris, A.C. Ferrari, M.S. Vitiello, M. Polini, Photodetectors based on graphene, other two-dimensional materials and hybrid systems, Nat. Nanotechnol. 9 (2014) 780–793, https://doi.org/10.1038/nnano.2014.215.

[55] D. Jariwala, A.R. Davoyan, J. Wong, H.A. Atwater, Van der Waals materials for atomically-thin photovoltaics: promise and outlook, ACS Photonics 4 (2017) 2962–2970, https://doi.org/10.1021/acsphotonics.7b01103.

[56] Q. Lu, Y. Yu, Q. Ma, B. Chen, H. Zhang, 2D transition-metal-dichalcogenide-nanosheet-based composites for photocatalytic and electrocatalytic hydrogen

evolution reactions, Adv. Mater. 28 (2016) 1917–1933, https://doi.org/10.1002/adma.201503270.
[57] D. Jariwala, A.R. Davoyan, G. Tagliabue, M.C. Sherrott, J. Wong, H.A. Atwater, Near-unity absorption in van der Waals semiconductors for ultrathin optoelectronics, Nano Lett. 16 (2016) 5482–5487, https://doi.org/10.1021/acs.nanolett.6b01914.
[58] Y. Zhao, S. Zhang, R. Shi, G.I.N. Waterhouse, J. Tang, T. Zhang, Two-dimensional photocatalyst design: a critical review of recent experimental and computational advances, Mater. Today 34 (2020) 78–91, https://doi.org/10.1016/j.mattod.2019.10.022.
[59] X. Guo, Q. Li, Y. Liu, T. Jin, Y. Chen, L. Guo, T. Lian, Enhanced light-driven charge separation and H 2 generation efficiency in WSe 2 nanosheet–semiconductor nanocrystal heterostructures, ACS Appl. Mater. Interfaces 12 (2020) 44769–44776, https://doi.org/10.1021/acsami.0c12931.
[60] C. Martella, C. Mennucci, A. Lamperti, E. Cappelluti, F.B. de Mongeot, A. Molle, Designer shape anisotropy on transition-metal-dichalcogenide nanosheets, Adv. Mater. 30 (2018), https://doi.org/10.1002/adma.201705615, 1705615–1705615.
[61] N. Yu, F. Capasso, Flat optics with designer metasurfaces, Nat. Mater. 13 (2014) 139–150, https://doi.org/10.1038/nmat3839.
[62] M. Bhatnagar, M.C. Giordano, C. Mennucci, D. Chowdhury, A. Mazzanti, G. Della Valle, C. Martella, P. Tummala, A. Lamperti, A. Molle, F. Buatier de Mongeot, Ultra-broadband photon harvesting in large-area few-layer MoS 2 nanostripe gratings, Nanoscale (2020), https://doi.org/10.1039/D0NR06744J.
[63] M. Bhatnagar, M. Gardella, M.C. Giordano, D. Chowdhury, C. Mennucci, A. Mazzanti, G. Della Valle, C. Martella, P. Tummala, A. Lamperti, A. Molle, F. Buatier de Mongeot, Broadband and tunable light harvesting in nanorippled MoS 2 ultrathin films, ACS Appl. Mater. Interfaces 13 (2021) 13508–13516, https://doi.org/10.1021/acsami.0c20387.
[64] A. Camellini, C. Mennucci, E. Cinquanta, C. Martella, A. Mazzanti, A. Lamperti, A. Molle, F.B. de Mongeot, G. Della Valle, M. Zavelani-Rossi, Ultrafast anisotropic exciton dynamics in nanopatterned MoS $_2$ sheets, ACS Photonics 5 (2018) 3363–3371, https://doi.org/10.1021/acsphotonics.8b00621.
[65] A. Camellini, A. Mazzanti, C. Mennucci, C. Martella, A. Lamperti, A. Molle, F. Buatier de Mongeot, G. Della Valle, M. Zavelani-Rossi, Evidence of plasmon enhanced charge transfer in large-area hybrid Au–MoS 2 metasurface, Adv. Opt. Mater. 8 (2020), 2000653, https://doi.org/10.1002/adom.202000653.
[66] Y.-M. He, G. Clark, J.R. Schaibley, Y. He, M.-C. Chen, Y.-J. Wei, X. Ding, Q. Zhang, W. Yao, X. Xu, C.-Y. Lu, J.-W. Pan, Single quantum emitters in monolayer semiconductors, Nat. Nanotechnol. 10 (2015) 497–502, https://doi.org/10.1038/nnano.2015.75.
[67] A. Castellanos-Gomez, R. Roldán, E. Cappelluti, M. Buscema, F. Guinea, H.S.J. van der Zant, G.A. Steele, Local strain engineering in atomically thin MoS $_2$, Nano Lett. 13 (2013) 5361–5366, https://doi.org/10.1021/nl402875m.
[68] C. Chakraborty, L. Kinnischtzke, K.M. Goodfellow, R. Beams, A.N. Vamivakas, Voltage-controlled quantum light from an atomically thin semiconductor, Nat. Nanotechnol. 10 (2015) 507–511, https://doi.org/10.1038/nnano.2015.79.
[69] T.E. Northup, R. Blatt, Quantum information transfer using photons, Nat. Photonics 8 (2014) 356–363, https://doi.org/10.1038/nphoton.2014.53.
[70] A. Dasgupta, J. Gao, X. Yang, Atomically thin nonlinear transition metal dichalcogenide holograms, Nano Lett. 19 (2019) 6511–6516, https://doi.org/10.1021/acs.nanolett.9b02740.
[71] J. Yang, Z. Wang, F. Wang, R. Xu, J. Tao, S. Zhang, Q. Qin, B. Luther-Davies, C. Jagadish, Z. Yu, Y. Lu, Atomically thin optical lenses and gratings, Light Sci. Appl. 5 (2016), e16046–e16046, https://doi.org/10.1038/lsa.2016.46.
[72] H. Lin, Z.-Q. Xu, G. Cao, Y. Zhang, J. Zhou, Z. Wang, Z. Wan, Z. Liu, K.P. Loh, C.-W. Qiu, Q. Bao, B. Jia, Diffraction-limited imaging with monolayer 2D material-based ultrathin flat lenses, Light Sci. Appl. 9 (2020) 137, https://doi.org/10.1038/s41377-020-00374-9.
[73] H. Zeng, J. Dai, W. Yao, D. Xiao, X. Cui, Valley polarization in MoS2 monolayers by optical pumping, Nat. Nanotechnol. 7 (2012) 490–493, https://doi.org/10.1038/nnano.2012.95.
[74] K. Rong, B. Wang, A. Reuven, E. Maguid, B. Cohn, V. Kleiner, S. Katznelson, E. Koren, E. Hasman, Photonic Rashba effect from quantum emitters mediated by a Berry-phase defective photonic crystal, Nat. Nanotechnol. 15 (2020) 927–933, https://doi.org/10.1038/s41565-020-0758-6.
[75] C. Mennucci, A. Mazzanti, C. Martella, A. Lamperti, M. Bhatnagar, R. Lo Savio, L. Repetto, A. Camellini, M. Zavelani-Rossi, A. Molle, F. Buatier de Mongeot, G. Della Valle, Geometrical engineering of giant optical dichroism in rippled MoS 2 nanosheets, Adv. Opt. Mater. (2020), 2001408, https://doi.org/10.1002/adom.202001408.
[76] P. Di Pietro, M. Ortolani, O. Limaj, A. Di Gaspare, V. Giliberti, F. Giorgianni, M. Brahlek, N. Bansal, N. Koirala, S. Oh, P. Calvani, S. Lupi, Observation of Dirac plasmons in a topological insulator, Nat. Nanotechnol. 8 (2013) 556–560, https://doi.org/10.1038/nnano.2013.134.
[77] L. Ju, B. Geng, J. Horng, C. Girit, M. Martin, Z. Hao, H.A. Bechtel, X. Liang, A. Zettl, Y.R. Shen, F. Wang, Graphene plasmonics for tunable terahertz metamaterials, Nat. Nanotechnol. 6 (2011) 630–634, https://doi.org/10.1038/nnano.2011.146.
[78] J.-C. Deinert, D. Alcaraz Iranzo, R. Pérez, X. Jia, H.A. Hafez, I. Ilyakov, N. Awari, M. Chen, M. Bawatna, A.N. Ponomaryov, S. Germanskiy, M. Bonn, F.H.L. Koppens, D. Turchinovich, M. Gensch, S. Kovalev, K.-J. Tielrooij, Grating-graphene metamaterial as a platform for terahertz nonlinear photonics, ACS Nano 15 (2021) 1145–1154, https://doi.org/10.1021/acsnano.0c08106.
[79] S. Lupi, A. Molle, Emerging Dirac materials for THz plasmonics, Appl. Mater. Today. 20 (2020), 100732, https://doi.org/10.1016/j.apmt.2020.100732.